Thermal infrared spectroscopy of experimentally shocked anorthosite and pyroxenite: Implications for remote sensing of Mars

Jeffrey R. Johnson,[1] Friedrich Hörz,[2] Paul G. Lucey,[3] and Philip R. Christensen[4]

Received 15 May 2001; revised 4 February 2002; accepted 22 April 2002; published XX Month 2002.

[1] The feldspar and pyroxene mineralogies on Mars revealed by the Thermal Emission Spectrometer (TES) on Mars Global Surveyor likely record a variety of shock effects, as suggested by petrologic analyses of the Martian meteorites and the abundance of impact craters on the planet's surface. To study the effects of shock pressures on thermal infrared spectra of these minerals, we performed shock recovery experiments on orthopyroxenite and anorthosite samples from the Stillwater Complex (Montana) over peak pressures from 17 to 63 GPa. We acquired emissivity and hemispherical reflectance spectra (350–1400 cm^{-1}; ~7–29 μm) of both coherent chips and fine-grained powders of shocked and unshocked samples. These spectra are more directly comparable to remotely sensed data of Mars (e.g., TES) than previously acquired absorption or transmission spectra of shocked minerals. The spectra of experimentally shocked feldspar show systematic changes with increasing pressure due to depolymerization of the silica tetrahedra. For the spectra of chips, this includes the disappearance of small bands in the 500–650 cm^{-1} region and a strong band at 1115 cm^{-1}, and changes in positions of a strong band near 940 cm^{-1} and the Christiansen feature near 1250 cm^{-1}. Spectra of the shocked powders show the gradual disappearance of a transparency feature near 830 cm^{-1}. Fewer changes are observed in the pyroxene spectra at pressures as high as 63 GPa. Spectra of experimentally shocked minerals will help identify more precisely the mineralogy of rocks and soils not only from TES but also from future Mars instruments such as miniTES and THEMIS. *INDEX TERMS:* 3944 Mineral Physics: Shock wave experiments; 3934 Mineral Physics: Optical, infrared, and Raman spectroscopy; 5420 Planetology: Solid Surface Planets: Impact phenomena (includes cratering); 5460 Planetology: Solid Surface Planets: Physical properties of materials; *KEYWORDS:* Anorthosite; pyroxenite; shock; spectra, thermal infrared; remote sensing, Mars

Citation: Johnson, J. R., F. Hörz, P. G. Lucey, and P. R. Christensen, Thermal infrared spectroscopy of experimentally shocked anorthosite and pyroxenite: Implications for remote sensing of Mars, *J. Geophys. Res.*, *107*(0), XXXX, doi:10.1029/2001JE001517, 2002.

1. Introduction

[2] Thermal infrared spectra of the Martian surface acquired by the Thermal Emission Spectrometer (TES) on Mars Global Surveyor provide a means to identify and map the distribution of a wide variety of minerals [*Christensen et al.*, 1998, 2001]. Spectral deconvolution (unmixing) of TES data using the Arizona State University (ASU) mineral spectral library [*Christensen et al.*, 2000b] has revealed dominantly feldspar and pyroxene mineralogies with lesser amounts of sheet silicates and volcanic glass components [*Christensen et al.*, 1998, 2000c]. Derived compositions appear to vary regionally [*Bandfield et al.*, 2000a] and currently include discrete occurrences of crystalline hematite [*Christensen et al.*, 2000a] and indications of olivine-rich regions [e.g., *Hoefen and Clark*, 2001].

[3] Detailed petrologic analyses of the minerals and textures in Martian meteorites suggest that they have experienced a variety of shock pressures and impact events [e.g., *McSween*, 1994; *Nyquist et al.*, 2001]. The abundance of craters on Mars provide testimony to the high energies and intense shock pressures associated with the formation and subsequent geologic evolution of the Martian crust [e.g., *Strom et al.*, 1992; *Hartmann et al.*, 1999; *Barlow et al.*, 2000]. The effect of high shock pressures on thermal infrared spectra of common rock-forming minerals is both an additional complication to the deconvolution of TES data and a means by which highly shocked materials can be identified and mapped on Mars.

[4] Shock-induced disordering of crystal lattices alters thermal infrared spectral features in laboratory transmission and absorption spectra of quartz, feldspars, pyroxenes, and olivines [*Pollack and DeCarli*, 1969; *Estep et al.*, 1972;

[1]U.S. Geological Survey, Flagstaff, Arizona, USA.
[2]Johnson Space Center, Houston, Texas, USA.
[3]Hawaii Institute of Geophysics and Planetology, University of Hawaii, Honolulu, Hawaii, USA.
[4]Department of Geology, Arizona State University, Tempe, Arizona, USA.

0148-0227/02/2001JE001517$09.00

Stöffler and Hornemann, 1972; *Ostertag*, 1983; *Stöffler and Langenhorst*, 1994; *Hofmeister*, 1997]. Preliminary reflectance measurements of naturally shocked rocks from terrestrial impact craters demonstrated that the reduction in structure of spectral features with increasing shock pressures was apparent in quartz [*D'Aria and Garvin*, 1988; *Garvin et al.*, 1992; *Betts and Nash*, 1994]. However, little systematic, quantitative work using directional hemispherical reflectance and emission spectra has been published, particularly for experimentally shocked pyroxenes and feldspars. Such spectra are more directly comparable to remotely sensed data of Mars such as that provided by TES than are transmission or absorption spectra. An improved understanding of the thermal infrared spectral effects of high shock pressures is critical to identifying more precisely the mineralogy of rocks and soils using data not only from TES, but also from future Mars instruments such as the miniTES [*Squyres et al.*, 1998] and the multispectral imager THEMIS [*Christensen et al.*, 1999].

[5] To study the thermal infrared spectral effects of shock on pyroxene and feldspar, we experimentally shocked orthopyroxenite and anorthosite samples from the Stillwater Complex (Montana) at peak pressures from 17 to 63 GPa and we examined their hemispherical reflectance and emission spectra (350–1400 cm^{-1}; ~7–30 μm). The results show systematic changes with increasing pressure in feldspar spectra but little change in pyroxene spectra. Use of these spectra as additional end-members in deconvolution models of thermal infrared spectra [e.g., *Thomson and Salisbury*, 1993; *Ramsey and Christensen*, 1998] may permit detection and mapping of shocked materials on Mars [*Johnson et al.*, 2002].

2. Background

[6] As reviewed by *Stöffler and Langenhorst* [1994] and *Grieve et al.* [1996], petrologic investigations of naturally and experimentally shocked minerals correlate shock pressure levels with specific deformation features, such as planar deformations, diaplectic glass, high-pressure polymorphs, and complete melting. Similar analysis techniques have been applied to terrestrial crater materials [e.g., *Short*, 1970; *Dence et al.*, 1977], lunar regolith samples [e.g., *Hörz and Cintala*, 1997], and meteorites [e.g., *Stöffler et al.*, 1991; *Bischoff and Stöffler*, 1992] to understand better their thermal and shock metamorphic histories.

[7] Some of the first applications of reflectance spectroscopy to shocked materials were laboratory visible/near-infrared measurements of plagioclase and enstatite [*Adams et al.*, 1979; *Bruckenthal and Pieters*, 1984; *King*, 1986]. Few variations in spectral features with pressure were observed except for a decrease in the absorption feature near 1250 nm in plagioclase [cf. *Lucey*, 2002]. *Lambert* [1981] also measured the visible (589 nm) reflectivity of quartz and plagioclase polished thin section surfaces to estimate the variation of refractive index caused by shock pressures greater than ~20–25 GPa [cf. *Hörz*, 1968; *Stöffler*, 1974; *Stöffler and Langenhorst*, 1994].

[8] Previous thermal infrared spectral studies of experimentally and naturally shocked materials concentrated on transmission and absorption spectra. Reflectance and emission spectroscopy of shocked materials is preferable to those techniques because of its current use as both a laboratory and remote sensing tool. Further, reflectance and emittance spectra depend on both the absorption coefficient and refractive index, whereas transmission/absorption spectra depend mainly on the absorption coefficient [e.g., *Salisbury et al.*, 1991b]. This causes potentially significant spectral features apparent in reflectance and emittance spectra to be absent or reduced in transmittance spectra.

[9] *Lyon* [1963] and *Bunch et al.* [1968] were among the first to note that increasing shock pressures cause a decrease in the spectral detail and intensity of absorption features in quartz and feldspars. This behavior was attributed to the increased disorder of the lattice structure in the shocked minerals. *Stöffler* [1972, 1974] and *Stöffler and Hornemann* [1972] obtained infrared absorption spectra of naturally and experimentally shocked quartz and feldspars that showed a decrease in the number and sharpness of absorptions and shifts in band positions as pressure increased. *Schneider* [1978] suggested that pressures higher than 18 GPa in experimentally shocked quartz increased the amount of diaplectic glass and caused characteristic changes in absorption features. Infrared absorption studies on experimentally shocked feldspars indicated weakening and shifts in absorption bands related to increasing glass content, particularly at shock pressures above ~20 GPa [*Arndt et al.*, 1982; *Ostertag*, 1983; *Nash and Salisbury*, 1991; *Williams*, 1998]. Diaplectic glass ("maskelynite") formation in feldspars occurs between ~30–45 GPa, while significant melting occurs above ~42 GPa [*Stöffler*, 1972; *Gibbons et al.*, 1975; *Hörz and Cintala*, 1997; *Velde et al.*, 1987, 1989], although the absolute strain rate, absolute stress, and shock pulse duration likely influence the precise shock levels for melting [*Stöffler*, 2001; *DeCarli et al.*, 2001]. Infrared absorption spectra of olivines subjected to high pressures exhibit spectral features that are broader and shifted to higher wave numbers relative to ambient conditions, indicative of increasing disorder [*Schneider and Hornemann*, 1977; *Hofmeister et al.*, 1989; *Hofmeister*, 1997; *Wang et al.*, 1993].

[10] Transmission spectra of shocked orthopyroxenes obtained by *Estep et al.* [1972] showed little change in spectral features until >45 GPa. This is consistent with early X-ray and Mössbauer spectra of shocked pyroxenes that showed structural disorder did not occur in enstatites until >45 GPa [*Pollack and DeCarli*, 1969; *Dundon and Hafner*, 1971; *Hörz and Quaide*, 1973]. Other work also has suggested that pyroxenes are relatively resilient to high shock pressures and mainly show only mechanical defects (fractures, lattice dislocations, twinning, planar deformation features) up to ~45 GPa or more [*Ahrens and Gaffney*, 1971; *Stöffler et al.*, 1991; *Leroux et al.*, 1994; *Schmitt and Deutsch*, 1995; *Kotelnikov and Feldman*, 1998], and that significant melting may not begin until >60 GPa [e.g., *Stöffler*, 1972; *Stöffler et al.*, 1991; *Hörz and Cintala*, 1997; *Xie et al.*, 2001]. However, the rarefaction and reflection of shock waves across grain boundaries often results in a heterogeneous distribution of shock pressures in sample volumes as small as 1 cm^3 [e.g., *Hanss et al.*, 1978]. This can result in minor localized melting along grain boundaries at pressures lower

than 50 GPa in pyroxenes [e.g., *Feldman et al.*, 1994; *Sazonova et al.*, 1996].

3. Methodology

3.1. Shock Experiments and Samples

[11] The shock experiments were performed with the Flat Plate Accelerator, a powder propellant gun, at the Johnson Space Center, Houston. This launches flat metal plates for the production of planar shock waves in targets of geologic interest [cf. *Gibbons et al.*, 1975; *Cygan et al.*, 1992]. Salient experimental details are summarized in Table 1. The projectile was a lexan-cylinder faced with a flat, metallic "flyer" plate of diameter 22 mm and thickness T_p (typically 2 mm). The geologic target was a disc cored from the rock sample, 12 mm in diameter and 1 mm thick. A few experiments were conducted with a 20 mm barrel using target disks of 7 × 0.5 mm (see Table 1). This target disc was effectively encapsulated into a metal jacket. This jacket in turn was housed in a substantial target "holder", machined from identical materials as the jacket. This massive holder was placed inside the impact chamber (maintained at 10^{-3} atm during the actual impact) and held in the path of the projectile by 3 plastic screws. The screws broke upon impact, allowing the entire holder to move freely, and thus providing for an efficient momentum trap. All dimensions of the machined target parts were scaled toward those of the flyer plate thickness (T_p) to assure that the geologic target equilibrated with its surrounding metal jacket within timescales commensurate with the pulse duration (t) of the shock wave ($t = T_p/U_s$ where U_s = shock wave velocity). Using millimeter-sized flyer plates produced pulse durations in the present experiments on the order of a few microseconds. By manufacturing the flyer plate and all target assembly and holder parts from materials with known equations of state (EOS), a graphical impedance match method could be applied to solve for the shock peak pressure at the projectile/target interface [e.g., *Duvall*, 1962]. Trade-offs between impact speed and the acoustic impedance of the materials used for the flyer plate and target assembly were made to vary the peak pressure in these experiments (Table 1). The impact velocity was measured in the Flat Plate Accelerator via laser occultation methods to a precision of 0.5%.

[12] Following an experiment, the target-holder, including the jacket-assembly inserted in its front, was recovered in relatively undeformed condition. A lathe was used, employing gaseous N_2 as a coolant, to remove excess metal until the silicate target could be pried from its original target well. Careful prying allowed for the recovery of relatively large chips (2–10 mm) that were separated from the more fine-grained materials. The latter were gently powdered to a more homogeneous grain size (<20–30 μm). Unshocked samples also were similarly powdered and broken into smaller chips for better comparison to the shocked samples. Use of the 20 and 25 mm barrels allowed for different target sizes and recovered mass (60 and 400 mg, respectively).

[13] The small target-discs may readily be manufactured from single crystal feldspars or pyroxenes, but we used polycrystalline and essentially monomineralic rocks in this work to avoid possible bias of crystal-lattice orientation relative to the propagating shock on the type and degree of shock deformation. This required target rocks of millimeter-sized crystals of random orientations. Samples that fit these criteria were acquired from the Stillwater Complex (Montana), an igneous layered intrusion containing orthopyroxenite and anorthositic rocks that have been studied by both terrestrial and planetary science communities [e.g., *Hess*, 1960; *Jackson*, 1961; *Page*, 1977; *Papike et al.*, 1995]. The Stillwater orthopyroxenites and anorthosites are relevant to the specific pyroxene and feldspar mineralogies identified by TES on Mars as well as the orthopyroxene-rich shergottites in the Martian meteorite collection [*McSween*, 1994]. Other pyroxenites have been well-studied, particularly in comparison to the Martian meteorites (e.g., Theo's Flow in Canada [*Friedman et al.*, 1995; *Treiman et al.*, 1996]) but do not contain abundant (>80%) pyroxene. We chose an anorthosite with ~90% bytownite (An_{75}), ~5 clinopyroxene, and ~5% orthopyroxene from the AN-II unit of the Middle Banded Series [*Haskin and Salpas*, 1992] to represent the feldspar. We chose an orthopyroxenite with ~90% bronzite (En_{85}), interstitial plagioclase (~8%) and clinopyroxene (~2%) from the Peridotite Zone of the Ultramafic Series [*Raedeke and McCallum*, 1984] to represent the pyroxene.

Table 1. Detailed Experimental Conditions for the Shock Recovery Experiments of Anorthosite and Pyroxenite Targets

EIL Number[a]	Target	Impact Velocity, km/s	Flyer Plate[b]	Assembly	Peak Pressure, GPa
3156	Plag.	1.344	Al2024	SS304	17.0
3154	Plag.	1.001	SS304	SS304	21.0
3151	Plag.	1.021	SS304	SS304	21.5
3155	Plag.	1.061	SS304	SS304	22.6
3146	Plag.	1.182	SS304	SS304	25.5
3145	Plag.	1.243	SS304	SS304	27.0
3142	Plag.	1.333	SS304	SS304	29.3
3148	Plag.	1.301	SS304	FS77	37.5
3143	Plag.	1.325	SS304	FS77	38.2
3149	Plag.	1.233	FS77	FS77	49.2
3144	Plag.	1.385	FS77	FS77	56.3
3214	Opx	1.391	Al2024	SS304	19.0
3257	Opx	1.171	SS304	SS304	25.2
3208	Opx	1.377	SS304	SS304	30.5
3258	Opx	1.234	SS304	FS77	35.0
3215	Opx	1.389	SS304	FS77	40.0
3218	Opx	1.109	SS304	FS77	43.9
3268[c]	Opx	1.369	W	FS77	59.6
3266[c]	Opx	1.385	W	FS77	60.0
3267[c]	Opx	1.385	W	FS77	60.0
3265[c]	Opx	1.420	W	FS77	62.1
3270[c]	Opx	1.434	W	FS77	62.9

[a] Running Flat Plate Accelerator experiment number in Experimental Impact Laboratory at JSC.

[b] Projectile and assembly materials (EOS): Aluminum2024 [*Marsh*, 1980], Stainless Steel 304 [*Marsh*, 1980], "Fansteel 77" (a W-Ni alloy [*Jones et al.*, 1966]), W = pure tungsten [*Marsh*, 1980].

[c] Experiments employing the 20 mm barrel and 18 mm diameter flyer plates; all other experiments were conducted with the 25 mm barrel and 23 mm diameter flyer plates; all flyer plates were 2 mm thick, except for the W plates (1 mm). Note: shots 3266 through 3268 and shots 3265 and 3270 were combined into two samples of sufficient mass to conduct the optical measurements and assigned average peak pressures of 59.9 and 62.5 GPa, respectively.

3.2. Thermal Infrared Spectroscopy

[14] Infrared spectrometers at the University of Hawaii (UH) and Arizona State University (ASU) were used to obtain directional hemispherical reflectance and emissivity spectra of the larger chips and powders. Spectra of powders packed with hand pressure were also acquired to determine

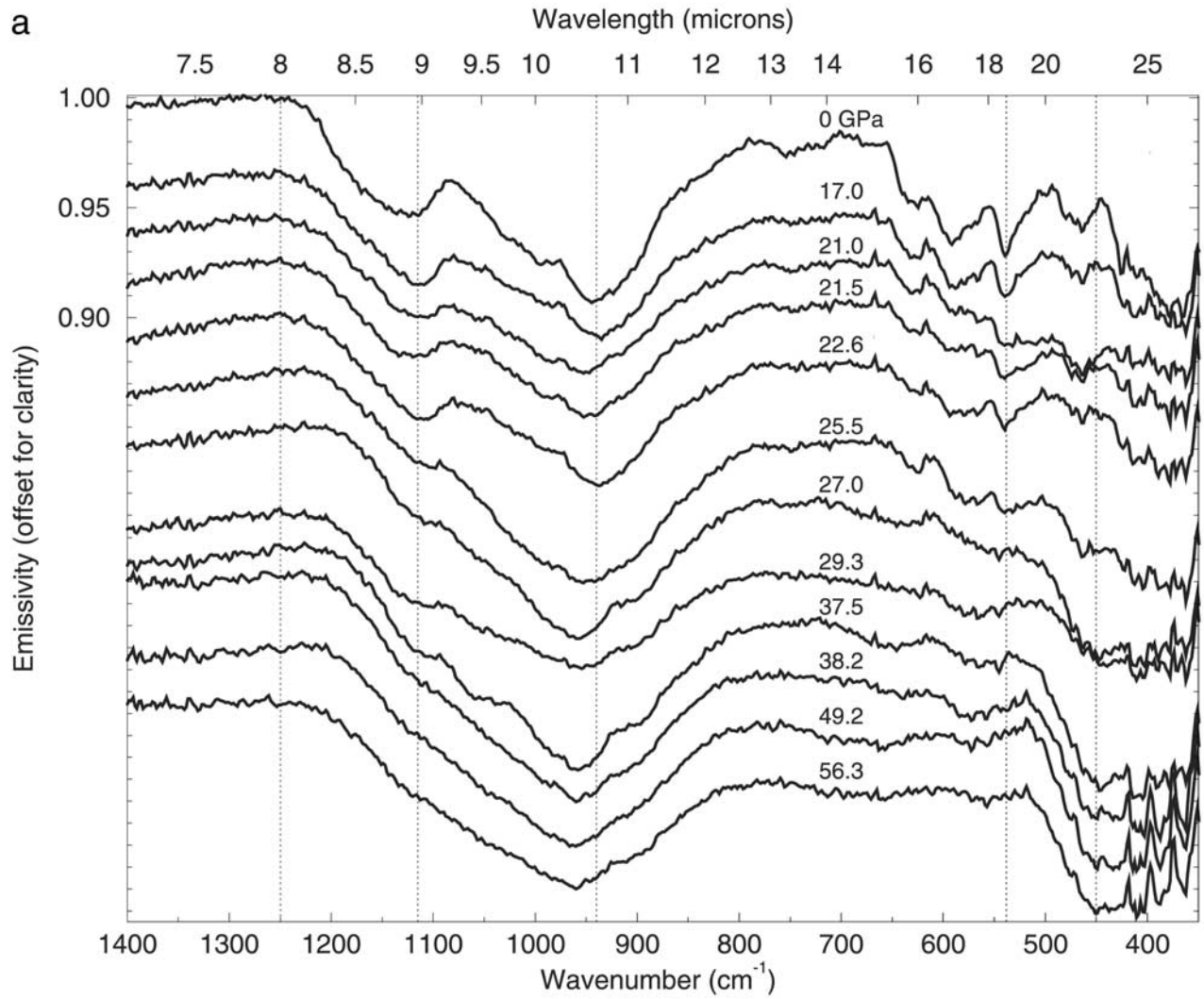

Figure 1. (a) Emissivity spectra of anorthosite chips recovered from shock experiments, with shock pressures labeled above each spectrum. (b) Hemispherical reflectance spectra (inverted to emissivity) of the anorthosite chips. Vertical dotted lines located where spectral features vary with increasing pressure: 1250, 1115, 940, 538, and 450 cm^{-1} (see text). All spectra are offset from the unshocked (0 GPa) spectrum in each plot.

the extent to which packing would improve spectral contrast for these samples [e.g., *Salisbury and Wald*, 1992; *Johnson et al.*, 1998]. Acquisition of spectra using both UH and ASU instruments allowed comparison of reflectance and emission techniques and provide checks on the reproducibility of the results [cf. *Mustard and Hays*, 1997].

[15] The UH operates a Nicolet 740 spectrometer capable of providing directional hemispherical reflectance (715–3300 cm^{-1}; 3–14 μm) (similar to the arrangement of *Salisbury et al.* [1991a, 1991b, 1994]) in which the spectrometer's external port is fitted with an integrating sphere, coated inside with a diffusely reflecting gold surface, and a liquid nitrogen-cooled Hg-Cd-Te (MCT) detector [*Johnson et al.*, 1998]. The spectrometer was configured to provide 8 cm^{-1} resolution with 1000 scans co-added per sample spectrum, which was ratioed to the spectrum of a diffusely reflecting gold plate to provide a hemispherical reflectance spectrum. This type of spectrum allows direct conversion to emission spectra via Kirchhoff's law, unlike biconical reflectance spectra that are subject to anomalous scattering effects [*Salisbury*, 1993; *Salisbury et al.*, 1991a, 1991b, 1994]. Unfortunately, all but the unshocked samples were insufficient in size to fully cover the spectrometer's infrared field of view. To compensate for the small sample area we placed the samples on cups that were plated with the same reflective gold surface as the interior of the integrating sphere and that were sufficiently large to fill the sample port. This provided consistent measurements of a sample's spectral reflectance but at the expense of uncertainties in the absolute reflectance values because a portion of the "sample" viewed by the spectrometer was highly reflective, gold-plated sample cup. However, measurements of the larger unshocked samples that filled the sample port provided a baseline from which the shocked sample reflectance values could be scaled, and emissivity measurements of the same samples provided an additional check on the reflectance levels.

[16] ASU operates a Nicolet Nexus 670 spectrometer equipped with an uncooled deuterated triglycine sulfate

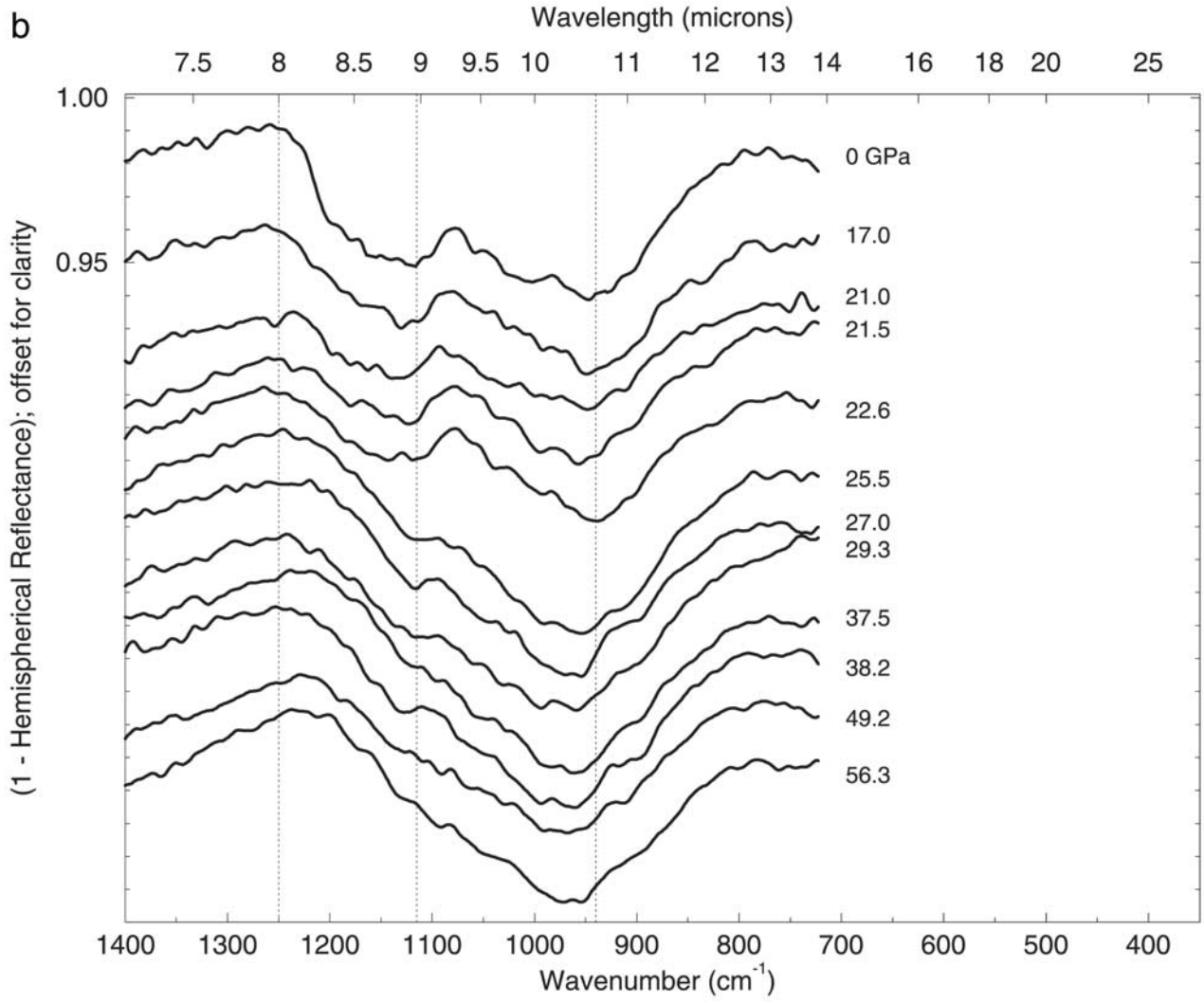

Figure 1. (continued)

(DTGS) detector adapted for emission spectroscopy [*Ruff et al.*, 1997]. Energy from a heated particulate sample (maintained at 80°C) is collected by a parabolic mirror and directed toward the interferometer, and blackbodies at 70°C and 100°C are used for radiometric calibration. For this instrument, the small sample size was compensated by adjusting the sample location within the optical path such that the infrared beam was confined to the sample. The spectrometer was configured to provide 4 cm^{-1} resolution from 1667–200 cm^{-1} (6–50 μm) with 180 to 250 scans co-added per spectrum. Although the enclosed system was purged continuously to remove CO_2 and water vapor, some of the spectra presented here were contaminated with sufficient residual water vapor at <350 cm^{-1} (29 μm) to prevent inclusion of that spectral region. As such, all spectra are presented below from 350–1400 cm^{-1} (7–29 μm).

4. Results

4.1. Anorthosite

[17] Emissivity and hemispherical reflectance spectra of the shocked anorthosite chips shown in Figure 1 demonstrate a variety of features that change with increasing shock pressure indicative of lattice disorders associated with the increasing formation of glass. A major absorption at 1115 cm^{-1} (9.0 μm) and smaller absorptions at 538 cm^{-1} (18.6 μm), 590 cm^{-1} (17.0 μm), and 630 cm^{-1} (15.9 μm) decrease in band strength. Figure 2 shows the correlation between the 1115 cm^{-1} band depth and pressure is linear in both emissivity and reflectance spectra. An absorption centered near 465 cm^{-1} (21.5 μm) disappears by 25.5 GPa and then develops into a broad band centered near 450 cm^{-1} (22.2 μm) at higher pressures, as shown in Figure 3. The Christiansen feature (CF) at ~1250 cm^{-1} (8.0 μm) shifts to smaller wave numbers with increasing pressure (Figure 4), whereas the position of the prominent 940 cm^{-1} (10.6 μm) band shifts slightly to higher wave numbers at higher pressures (Figure 5). Error bars used in Figures 4 and 5 represent the spectral resolutions of the emissivity and reflectance spectra and are used here because of the difficulty in precisely defining the positions of the CF and the 940 cm^{-1} band. The change in CF position varies slightly between emission and hemispherical reflectance spectra because of the different spectral resolutions of the two data sets [cf. *Salisbury et*

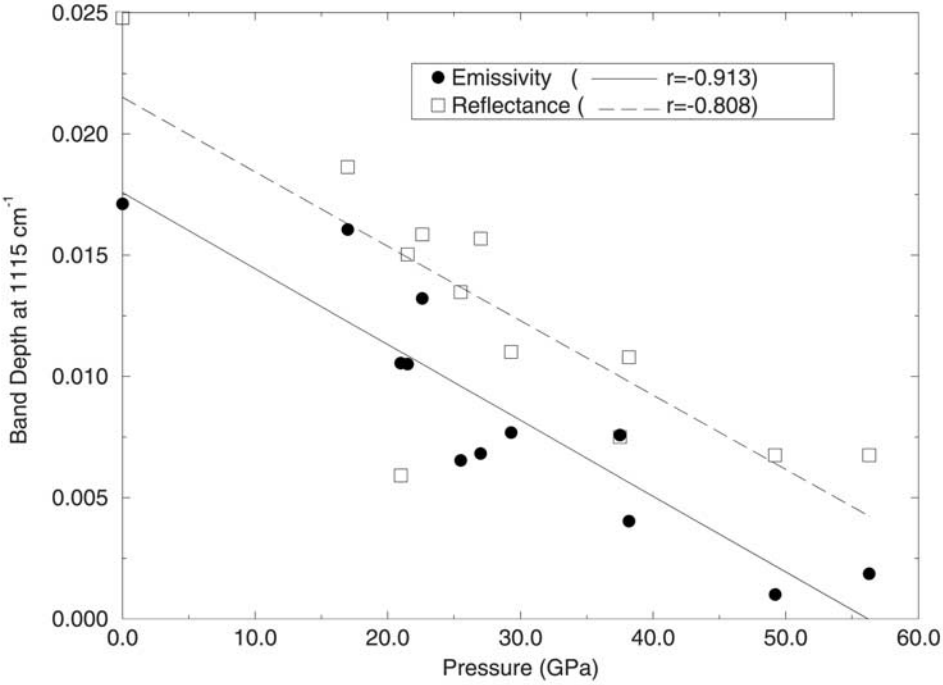

Figure 2. Band depth at 1115 cm^{-1} (computed using continuum between 1075 cm^{-1} and 1150 cm^{-1}) as a function of shock pressure for emissivity and hemispherical reflectance spectra of anorthosite chips. Linear correlation line and coefficients shown.

al., 1991a]. The CF positions observed for the unshocked anorthosite in both emissivity and reflectance data are still well within those observed for anorthite by *Nash and Salisbury* [1991].

[18] Figure 6 shows emissivity spectra of the shocked anorthosite powders. Reflectance spectra of these powders are quite similar, as are all spectra of packed powders, and are not shown here. In the powder spectra the bands at 1115 cm^{-1} and ~945 cm^{-1} are much more subdued than in the chip spectra (Figure 1). This is consistent with the powder's fine grain size [e.g., *Salisbury and Walter*, 1989], although a reduction in their band depths with increasing pressure is still noticeable. More apparent is the transparency band at 830 cm^{-1} (12.1 μm) caused by volume scattering [e.g., *Salisbury*, 1993]. This band also becomes more subdued with increasing pressure, as shown in Figure 7.

4.2. Pyroxenite

[19] Spectra of the pyroxenites show the characteristic "critical absorptions" (CA) described by *Hamilton* [2000] for orthopyroxenes, but little change in spectral features is observed for the pyroxenite chips even at pressures > 60 GPa (Figure 8). Minor absorptions at 976 cm^{-1} (10.3 μm) and 567 cm^{-1} (17.6 μm) (corresponding to CA2 and CA5, respectively, of *Hamilton* [2000]) degrade with increasing shock pressure. The stronger bands are more resilient to high shock pressures. This is consistent with results obtained from early transmission measurements of shocked pyroxenes [e.g., *Estep et al.*, 1972]. We note that minor differences among spectral features (e.g., CA shapes) may result from natural variations in the samples or differences in crystal orientations of the chips among the different samples [e.g., *Hamilton*, 2000].

[20] Emission spectra of shocked pyroxenite powders show little change with pressure as well (Figure 9). We note that spectra of powders shocked to 25.2, 35.0, 59.9 and 62.5 GPa were acquired as a separate subset of observations. These spectra are noisier and exhibit flatter spectral slopes at wave numbers > 1200 cm^{-1} than the other spectra. This is likely due to a combination of greater residual water vapor in these spectra and subtle differences in grain sizes produced during sample preparation. As such, the small transparency band at 800 cm^{-1} (12.5 μm) is only observed

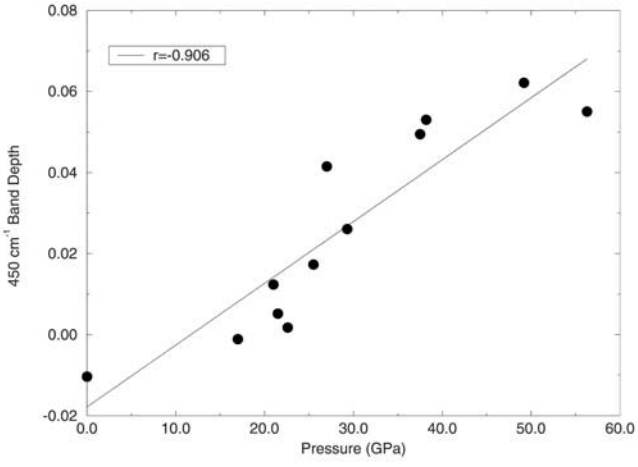

Figure 3. Band depth at 450 cm^{-1} (computed using continuum between 350 cm^{-1} and 520 cm^{-1}) as a function of shock pressure for emissivity spectra of anorthosite chips. Linear correlation line and coefficient shown.

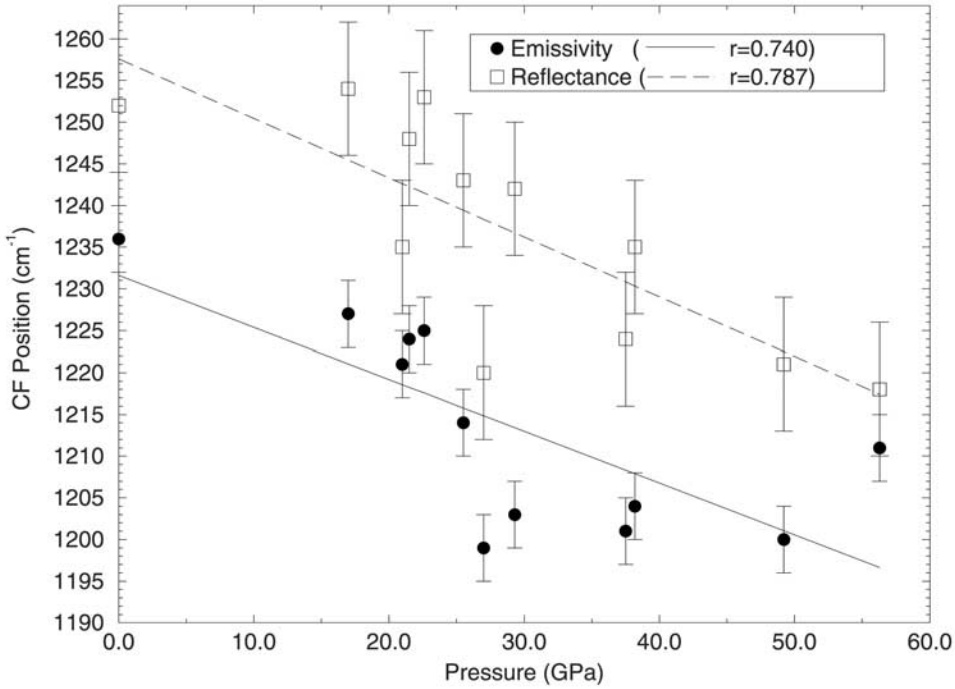

Figure 4. Changes in the position of the Christiansen feature (reflectance maximum, emissivity minimum [cf. *Salisbury*, 1993]) as a function of shock pressure for emissivity and hemispherical reflectance spectra of anorthosite chips. Error bars represent ± spectral resolution of measurements. Linear correlation lines and coefficients shown.

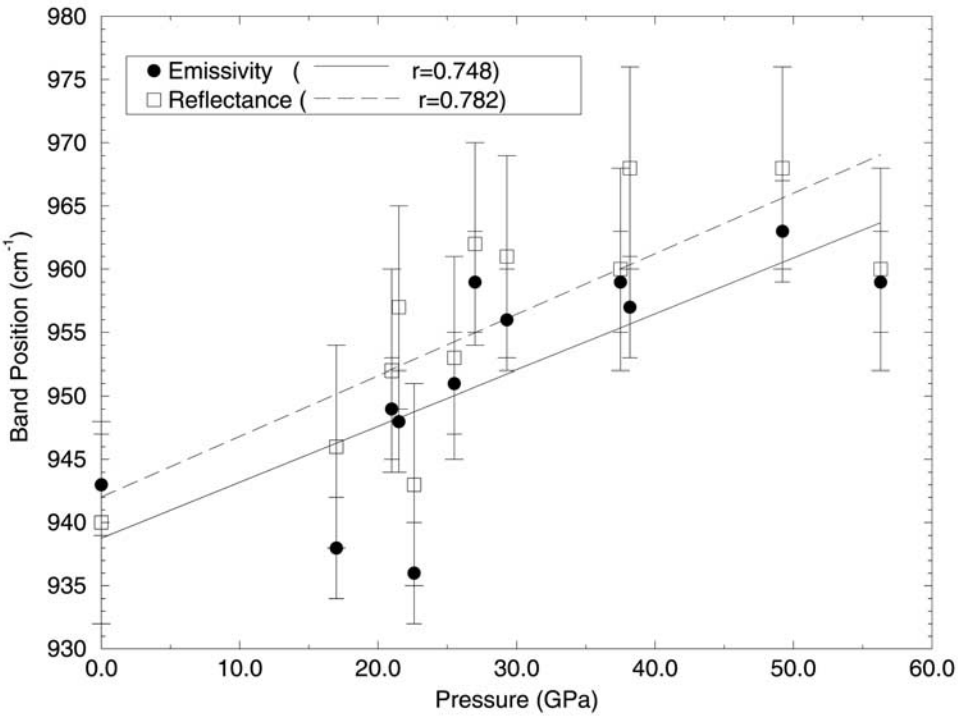

Figure 5. Changes in the position of the 940 cm^{-1} band as a function of shock pressure for emissivity and hemispherical reflectance spectra of anorthosite chips. Error bars represent ± spectral resolution of measurements. Linear correlation line and coefficients shown.

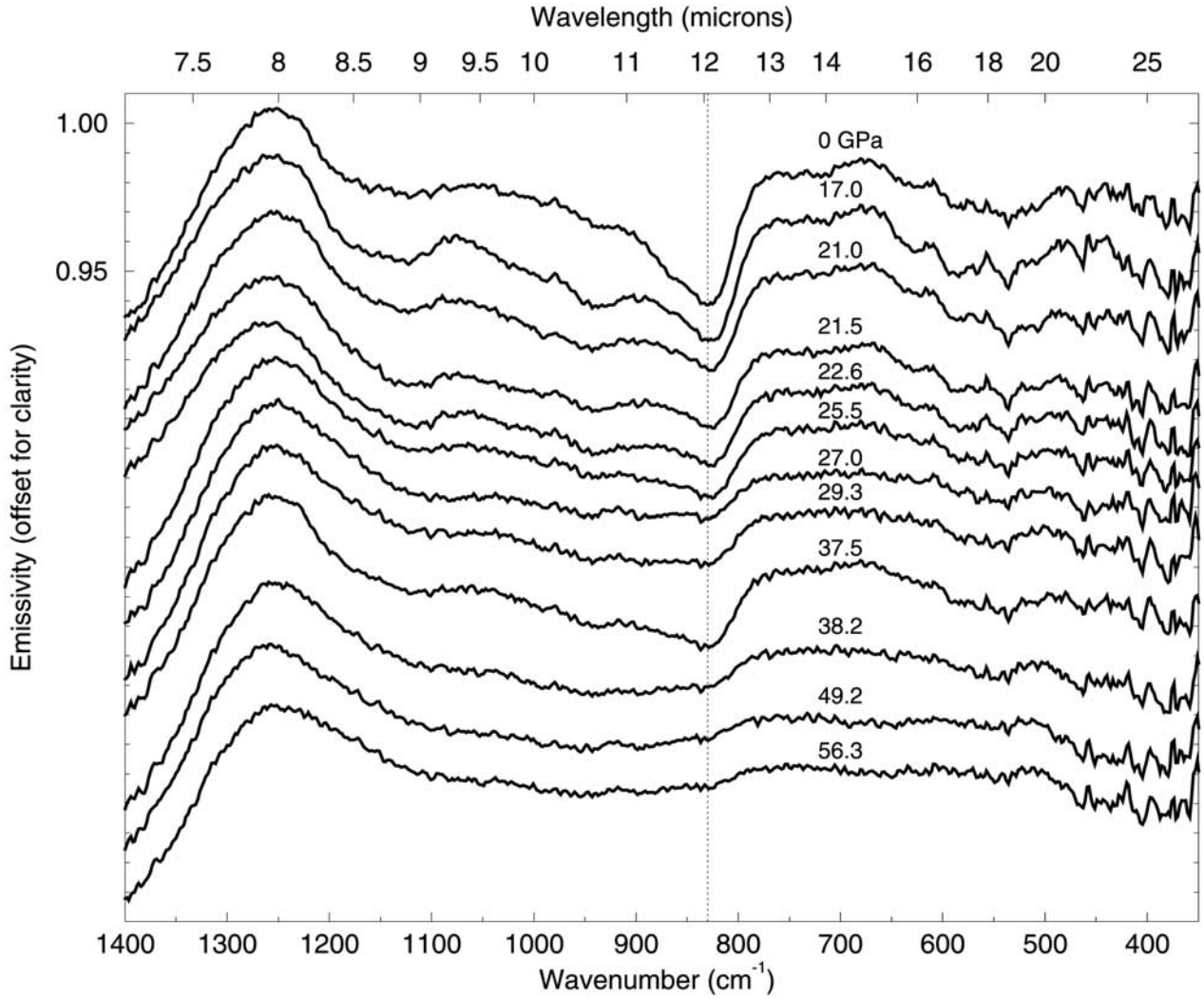

Figure 6. Emissivity spectra of anorthosite powders recovered from shock experiments, with shock pressures labeled above each spectrum. All spectra are offset from the unshocked (0 GPa) spectrum. Vertical dotted line at 830 cm^{-1} locates a transparency features that varies with increasing pressure as described in text.

in the less noisy and finer-grained powder spectra. Changes in the strength of this band appear more related to the effects of grain size and/or quality of spectra than to the effects of shock pressures. Again, reflectance spectra of these powders are very similar to their emissivity spectra, as are all spectra of packed powders, and are not shown here.

5. Discussion

5.1. Anorthosite

[21] The disordering effects on the crystalline structure of feldspars using both static (diamond anvil cells) and kinetic (shock recovery) high pressure experiments have been studied using dominantly infrared absorbance and Raman spectroscopy combined with x-ray diffraction [e.g., *Velde and Boyer*, 1985; *Velde et al.*, 1987, 1989; *Heymann and Hörz*, 1990; *Daniel et al.*, 1995, 1997; *Reynard et al.*, 1999]. Disordering of feldspar begins generally at pressures above 15–20 GPa and progressively increases until a dominantly amorphous state is reached by about 30 GPa

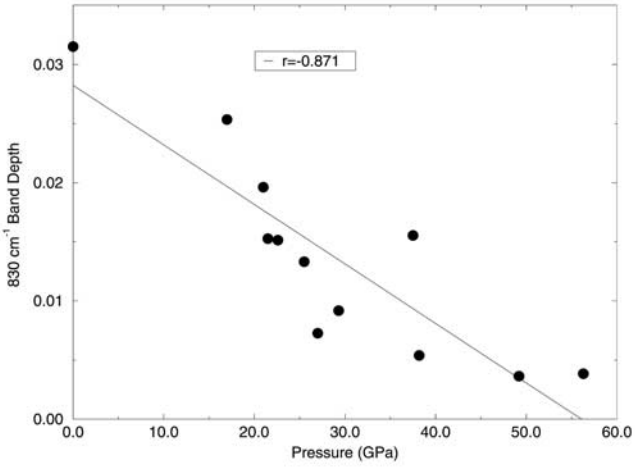

Figure 7. Band depth at 830 cm^{-1} (computed using continuum between 790 cm^{-1} and 900 cm^{-1}) as a function of shock pressure for emissivity spectra of anorthosite powders. Linear correlation line and coefficient shown.

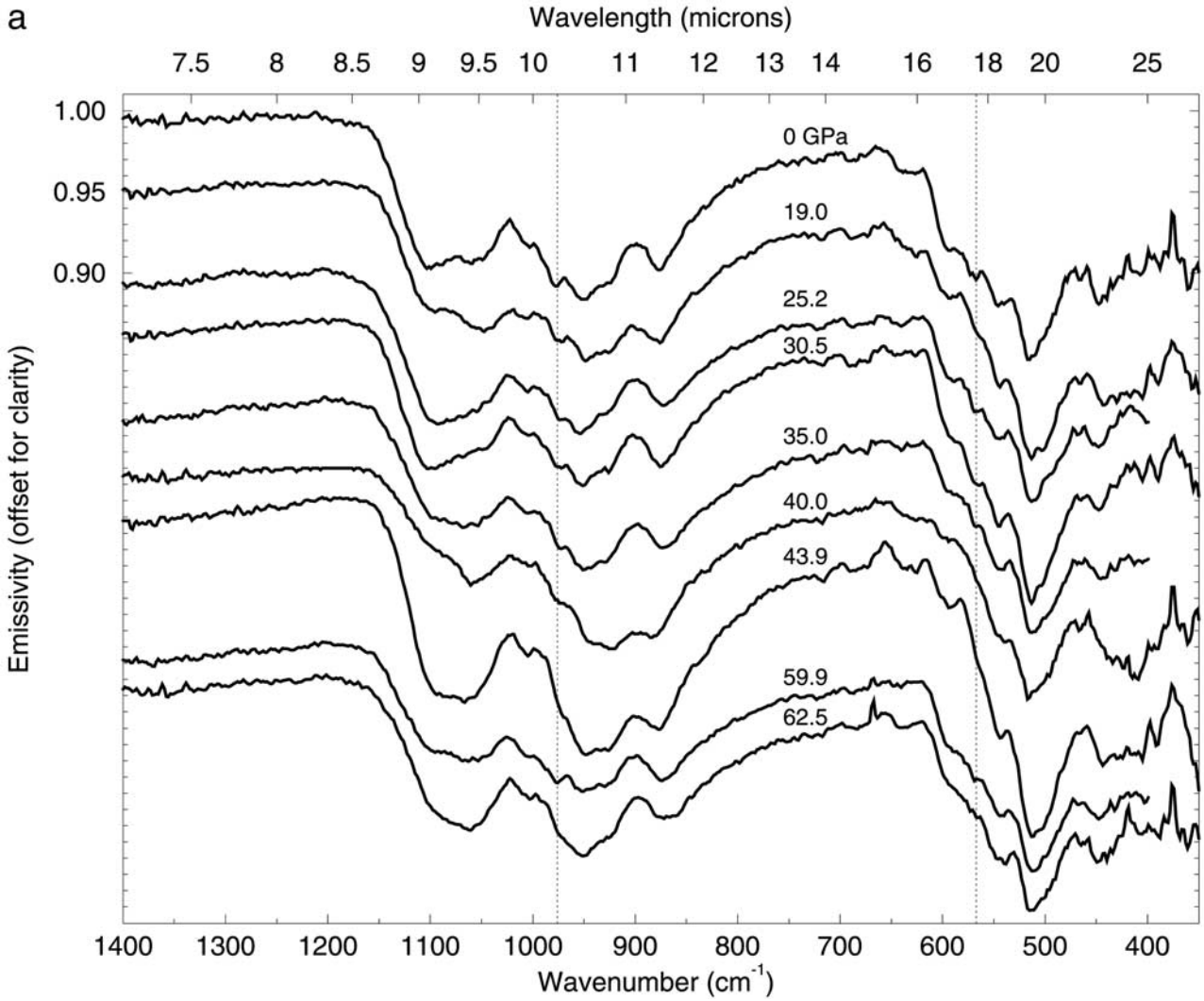

Figure 8. (a) Emissivity spectra of pyroxenite chips recovered from shock experiments, with shock pressures labeled above each spectrum. Spectra at 25.2, 35.0, and 59.9 GPa extend to only 400 cm^{-1} due to a software error during their acquisition. (b) Hemispherical reflectance spectra (inverted to emissivity) of the pyroxenite chips. Vertical dotted lines located at 976 cm^{-1} and 567 cm^{-1} where minor spectral features become more subdued with increasing pressure. All spectra are offset from the unshocked (0 GPa) spectrum in each plot.

[e.g., *Stöffler and Hornemann*, 1972; *Arndt et al.*, 1982; *Ostertag*, 1983; *Langenhorst*, 1989]. Within this pressure region the characteristic, fourfold (tetrahedral) strong coordination bonds of silicon and aluminum in feldspars distort to weaker, less polymerized bonds that approach sixfold (octahedral) coordination. The increased structural disorder and density results in the mutual existence of crystalline phases and diaplectic glasses throughout this pressure region which provide characteristic vibrational frequencies in the thermal infrared. Absorptions in the 900–1200 cm^{-1} region are due to Si-O antisymmetric stretch motions of the silica tetrahedral units in the structure. SiO_6 octahedral stretching vibrations occur between 750–850 cm^{-1} whereas Si-O-Si octahedral bending vibrations cause several smaller absorptions between about 700–450 cm^{-1}. Between 400–550 cm^{-1} bending vibrations in the Si-Al-O planar ring structures in tectosilicates and diaplectic glasses occur [*Bunch et al.*, 1967; *Iiishi et al.*, 1971; *Stöffler and Hornemann*, 1972; *Arndt et al.*, 1982; *Velde et al.*, 1987; *Williams and Jeanloz*, 1988, 1989; *Daniel et al.*, 1995, 1997; *Williams*, 1998].

[22] In shocked samples crystalline and amorphous phases likely coexist as intimate mixtures with the proportion of diaplectic glass increasing with shock pressure [*Ostertag*, 1983; *Heymann and Hörz*, 1990; *Yamaguchi and Sekine*, 2000]. The spectral features of anorthosite that change with increasing peak shock pressure are summarized in Table 2. The disappearance of the small bands between 500–650 cm^{-1} by 25.5 GPa is due to the depolymerization of the silica tetrahedra [e.g., *Williams*, 1998]. This behavior is similar to that observed in transmission spectra of diaplectic laboradorite glass from Manicouagan crater by *Arndt et al.* [1982] and in absorption spectra of shocked feldspars by *Ostertag* [1983], as is the appearance of the

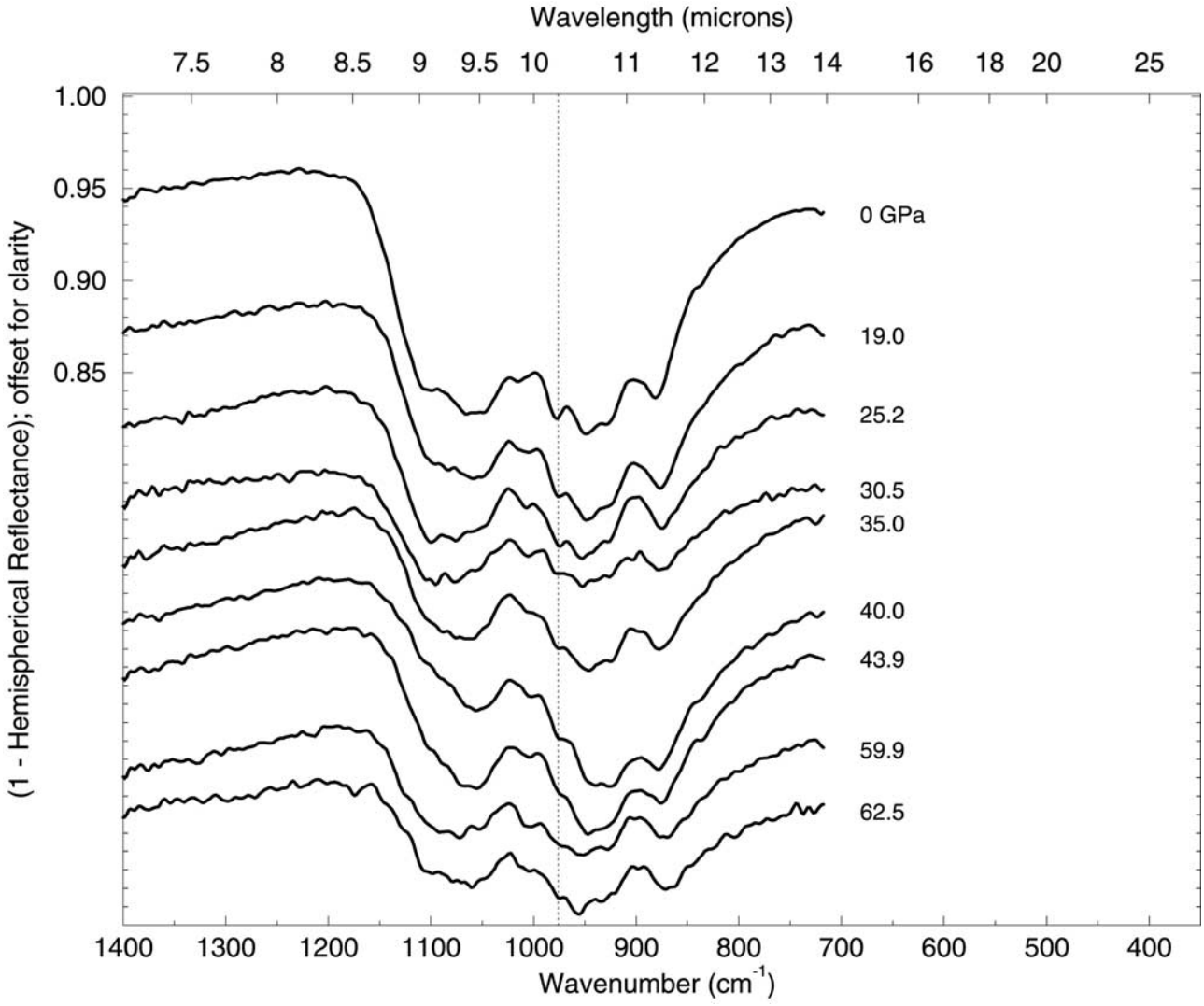

Figure 8. (continued)

band near 450 cm^{-1} with increasing pressure (Figure 1). For the stronger Si-O stretching bands, the higher-wave number band (1115 cm^{-1}) disappears by 38.2 GPa, and the lower-wave number band (940 cm^{-1}) shifts to higher wave numbers with pressure. These effects are similar to the feldspar observations of *Arndt et al.* [1982] and *Stöffler and Hornemann* [1972]. The shift in the Christiansen feature near 1250 cm^{-1} to lower wave numbers with increasing pressure in the chip samples (Figure 4) may be a side-effect of the loss of the 1115 cm^{-1} stretching band. The change in CF position is not observed in the powder sample spectra (Figure 6), consistent with results of *Nash and Salisbury* [1991] for biconical reflectance spectra of crystalline and fused powders of the same plagioclase composition.

[23] The transparency feature near 830 cm^{-1} in powdered samples (Figure 6) results from their fine grain size, which reduces the spectral contrast of the reststrahlen bands and allows volume scattering to dominate [e.g., *Salisbury et al.*, 1991a, 1991b]. The transparency feature disappears at high pressures, similar to the fused glass spectra of anorthite presented by *Nash and Salisbury* [1991]. This likely occurs because of the structural disorder in the highly shocked samples, which prevents significant volume scattering.

[24] Although transparency features can be difficult to detect on airless planetary surfaces due to severe temperature gradients [e.g., *Salisbury et al.*, 1991a, 1997], *Henderson and Jakosky* [1994] suggested that the atmospheric pressure on Mars is sufficient to minimize these effects. Indeed, although TES spectra of high albedo regions are dominantly blackbody-like (particularly in the reststrahlen region) [e.g., *Christensen et al.*, 2000c], ongoing analyses of some spectra reveal an absorption near 825 cm^{-1}, which is interpreted as a transparency feature associated with feldspar [e.g., *Ruff and Christensen*, 2002]. If this feature is absent in some high albedo regions, one explanation could be the presence of highly shocked, fine-grained feldspars. In support of this concept, we note that the similarity of impact melt compositions at Meteor Crater with Martian surface materials suggested to *Hörz et al.* [2002] that shock-produced glasses may be suitable analogs to some Martian surface materials. *Schultz and Mustard* [1998] came to similar conclusions upon comparison

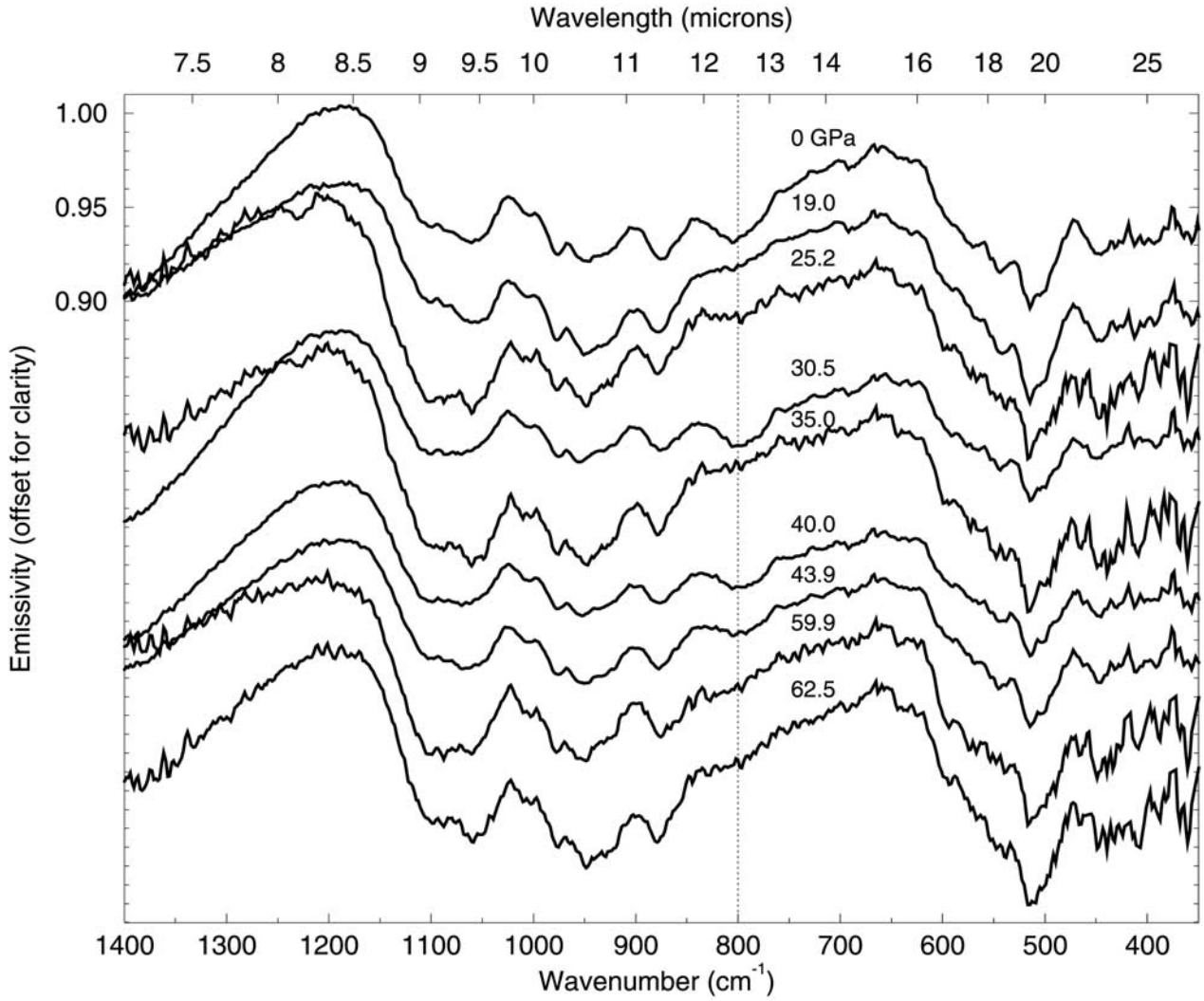

Figure 9. Emissivity spectra of pyroxenite powders recovered from shock experiments, with shock pressures labeled above each spectrum. All spectra are offset from the unshocked (0 GPa) spectrum. Vertical dotted line at 800 cm^{-1} locates a transparency features that varies as a function of grain size and data quality, as described in the text.

of visible/near-infrared spectra from Mars Pathfinder to spectra of glasses produced from impacts into terrestrial loess.

[25] Feldspar minerals with compositions other than the bytownite investigated here likely experience similar effects in their thermal infrared spectra at high shock pressures. Although differences in spectral detail of unshocked feldspars exist and are well documented [e.g., *Iiishi et al.*, 1971; *Nash and Salisbury*, 1991], *Ostertag* [1983] showed that changes in the thermal infrared transmission spectra of shocked feldspar crystals are very similar no matter the spectral shape of the unshocked samples. While the precise peak shock pressures at which structural disorder and melting occur may vary among feldspar compositions [e.g., *Williams*, 1998], the stretching and bending modes associated with Si-O, Si-O-Si, and Si-Al-O bonds generally weaken with increasing pressure and cause shifts in band positions similar to those observed here for bytownite. Emission and reflectance spectra of an experimentally shocked albite-rich rock are being acquired to test these observations and will be reported in a subsequent paper.

5.2. Pyroxenite

[26] In contrast to the multiple features in anorthosite spectra that provide sensitive barometers to shock pressure, the orthopyroxenite studied here shows little change in spectral properties with increasing pressure (Figures 8 and

Table 2. Summary of Observed Changes in Unshocked Spectral Feature Positions With Increasing Shock Pressure

Sample	Feature Position, cm^{-1}	Change With Increasing Pressure
Anorthosite (S2-104)	538, 590, 630, 1115	band depth decreases
	450	band depth increases
	940	band shifts to higher cm^{-1}
	1250	position shifts to lower cm^{-1}
	830 (powder)	band depth decreases
Orthopyroxenite (S-77)	976, 567	band depth decreases

9). The two minor bands at 976 cm^{-1} and 567 cm^{-1} degrade with increasing shock pressure, but the stronger bands maintain their relative depths and positions at high shock pressures. This is consistent with previous observations of shocked pyroxenes that demonstrated their resiliency and incompressibility to high pressures [e.g., *Ahrens and Gaffney*, 1971; *Dundon and Hafner*, 1971; *Stöffler et al.*, 1991; *Leroux et al.*, 1994; *Schmitt and Deutsch*, 1995].

[27] The disappearance of the small bands observed in the spectra here may result from minor amounts of melting similar to that observed in petrologic studies of samples shocked to pressures greater than about 45 GPa. Our spectra show that such melting apparently is insufficient to alter significantly the major stretching and bending vibration bands, at least to the maximum pressure of 62.5 GPa in the orthopyroxenite studied here. Indeed, *Estep et al.* [1972] required peak shock pressures of 100 GPa to observe a reduction in spectral detail in their transmission spectra.

[28] Although the only pyroxene composition we examined was bronzite, other pyroxenes probably also exhibit limited spectral changes over the range of shock pressures investigated here, as evidenced by numerous studies of both orthopyroxenes and clinopyroxenes which suggest that mechanical defects and fractures dominantly occur at these pressures [e.g., *Lambert*, 1982; *Sazonova et al.*, 1996; *Kotelnikov and Feldman*, 1998].

6. Conclusions

[29] Recognition of the spectral effects of high shock pressure on major rock forming minerals will aid understanding of remotely sensed thermal infrared surface spectra not only of Mars but of impact materials on the Earth, [e.g., *Ramsey and Christensen*, 1992], Moon [*Salisbury et al.*, 1995, 1997; *Nash et al.*, 1993], Mercury [*Sprague et al.*, 1992, 1994], asteroids such as 4 Vesta [e.g., *Morris et al.*, 1999], and shocked minerals in the SNC and lunar meteorites [*Hamilton et al.*, 1997; *Cooney et al.*, 1999; *Mikouchi*, 1999]. The new laboratory thermal infrared spectra presented here of shocked pyroxene- and feldspar-bearing rocks test the degree to which increased crystalline disorder caused by high shock pressures can be readily discerned using emission and directional hemispherical reflectance spectroscopy of particulate samples. Our results show that diagnostic spectral features change systematically with increasing pressure in high-calcium plagioclase feldspar, whereas very few features change in orthopyroxene to pressures of 62.5 GPa. Future spectroscopic studies will analyze experimentally shocked samples of other feldspar compositions (e.g., albite) plus basaltic and andesitic rocks (similar to those detected from TES spectra [e.g., *Bandfield et al.*, 2000a; *Hamilton et al.*, 2001; *Wyatt et al.*, 2001]). Raman spectroscopy of such samples also would be beneficial, particularly if this technique will be used for in situ measurements on Mars or if it can be developed as a remote-sensing tool [e.g., *Wang et al.*, 1999; *Horton et al.*, 2001].

[30] Unlike previous spectral studies of shocked minerals (transmission, absorption, biconical reflectance) the methods used here provide spectra that can be compared directly with remotely sensed surface spectra and can be incorporated as additional end-members in linear deconvolution methods to improve modeling and interpretation of TES data [e.g., Thomson and *Salisbury*, 1993; *Ramsey and Christensen*, 1998; *Bandfield et al.*, 2000b; *Hamilton and Christensen*, 2000]. In particular, the shocked feldspar spectra can be used in deconvolution models of TES spectra to help detect and map shocked materials located in impact ejecta on Mars to provide an additional means of interpreting the geology and provenance of impact materials [*Johnson et al.*, 2002]. Thus, the deconvolution of thermal infrared spectra such as that provided by TES (as well as future imaging systems such as THEMIS on the 2001 Mars Odyssey orbiter and miniTES on the 2003 Mars Exploration Rovers) should include shocked sample spectra such as that described here in mineral libraries.

[31] **Acknowledgments.** We thank K. Horton, C. Jensen, J. Linzi (Univ. Hawaii), V. Hamilton and S. Ruff (ASU) for assistance in acquiring the lab reflectance and emission spectra, J. Haynes (JSC) for performing the shock experiments, B. Jolliff and L. Haskin (Wash. Univ.) for the anorthosite sample, and S. McCallum (Univ. Washington) for the pyroxenite sample. Helpful reviews by M. Schaefer and P. Buchanan are appreciated, as is the editorial handling of A. Treiman. This work was performed under NASA contract W-19, 443 issued through the Planetary Geology and Geophysics Program.

References

Adams, J. B., F. Hörz, and R. V. Gibbons, Effects of shock-loading on the reflectance spectra of plagioclase, pyroxene, and glass, *Lunar Planet. Sci.*, *X*, 1–3, 1979.

Ahrens, T. J., and E. S. Gaffney, Dynamic compression of enstatite, *J. Geophys. Res.*, *76*, 5504–5513, 1971.

Arndt, J., W. Hummerl, and I. Gonzalez-Cabeza, Diaplectic Labradorite glass from the Manicouagan impact crater, I, Physical properties, crystallization, structural and genetic implications, *Phys. Chem. Miner.*, *8*, 230–239, 1982.

Bandfield, J. L., V. E. Hamilton, and P. R. Christensen, A global view of Martian surface compositions from MGS-TES, *Science*, *287*, 1626–1630, 2000a.

Bandfield, J. L., M. D. Smith, and P. R. Christensen, Spectral dataset factor analysis and end-member recovery: Application to analysis of Martian atmospheric particulates, *J. Geophys. Res.*, *105*, 9573–9587, 2000b.

Barlow, N. G., J. M. Boyce, F. M. Costard, R. A. Craddock, J. B. Garvin, S. E. Sakimoto, R. O. Kuzmin, D. J. Roddy, and L. A. Soderblom, Standardizing the nomenclature of Martian impact crater ejecta morphologies, *J. Geophys. Res.*, *105*, 26,733–26,738, 2000.

Betts, B. H., and D. B. Nash, Infrared spectra of shocked and unshocked Coconino sandstone from Meteor Crater, *Eos Trans. AGU*, *75*(44), Fall Meet., 416, 1994.

Bischoff, A., and D. Stöffler, Shock metamorphism as a fundamental process in the evolution of planetary bodies: Information from meteorites, *Eur.J. Mineral.*, *4*, 707–755, 1992.

Bruckenthal, E. A., and C. M. Pieters, Spectral effects of natural shock on plagioclase feldspar, *Lunar Planet. Sci.*, *XV*, 96–97, 1984.

Bunch, T. E., A. J. Cohen, and M. R. Dence, Natural terrestrial maskelynite, *Am. Mineral.*, *52*, 244–253, 1967.

Bunch, T. E., A. J. Cohen, and M. R. Dence, Shock-induced structural disorder in plagioclase and quartz, in *Shock Metamorphism of Natural Materials: Proceedings*, pp. 509–518, Mono Book, Baltimore, Md., 1968.

Christensen, P. R., et al., Results from the Mars Global Surveyor Thermal Emission Spectrometer, *Science*, *279*, 1692–1698, 1998.

Christensen, P. R., B. M. Jakosky, H. H. Kieffer, M. C. Malin, H. Y. McSween Jr., K. Nealson, G. Mehall, S. Silverman, and S. Ferry, The thermal emission imaging system (THEMIS) instrument for the Mars 2001 orbiter, *Lunar Planet. Sci.*, *XXX*, abstract 1470, 1999.

Christensen, P. R., et al., Detection of crystalline hematite mineralization on Mars by the Thermal Emission Spectrometer: Evidence for near-surface water, *J. Geophys. Res.*, *105*, 9623–9642, 2000a.

Christensen, P. R., J. L. Bandfield, V. E. Hamilton, D. A. Howard, M. D. Lane, J. L. Piatek, S. W. Ruff, and W. L. Stevanov, A thermal emission spectral library of rock-forming minerals, *J. Geophys. Res.*, *105*, 9735–9739, 2000b.

Christensen, P. R., J. L. Bandfield, M. D. Smith, V. E. Hamilton, and R. N.

Clark, Identification of a basaltic component on the Martian surface from Thermal Emission Spectrometer data, *J. Geophys. Res.*, *105*, 9609–9622, 2000c.
Christensen, P. R., et al., The Mars Global Surveyor Thermal Emission Spectrometer experiment: Investigation description and surface science results, *J. Geophys. Res.*, *106*, 23,823–23,871, 2001.
Cooney, T. F., E. R. D. Scott, A. N. Krot, S. K. Sharma, and A. Yamaguchi, Vibrational spectroscopic study of minerals in the Martian meteorite ALH84001, *Am. Mineral.*, *84*, 1569–1576, 1999.
Cygan, R. T., M. B. Boslough, and R. J. Kirkpatrick, NMR spectroscopy of experimentally shocked quartz and plagioclase powders, *Proc. Lunar Planet. Sci. Conf. 22nd*, 127–136, 1992.
D'Aria, D., and J. B. Garvin, Thermal infrared reflectance spectroscopy of impact-related rocks: Implications for geologic remote sensing of Mars and Earth, *Lunar Planet. Sci.*, *XIX*, 243–244, 1988.
Daniel, I., P. Gillet, and S. Ghose, A new high-pressure phase transition in anorthite ($CaAl_2Si_2O_8$) revealed by Raman spectroscopy, *Am. Mineral.*, *80*, 645–648, 1995.
Daniel, I., P. Gillet, P. F. McMillan, G. Wolf, and M. A. Verhelst, High-pressure behavior of anorthite: Compression and amorphization, *J. Geophys. Res.*, *102*, 10,313–10,325, 1997.
DeCarli, P. S., E. Bowden, T. G. Sharp, A. P. Jones, and G. D. Price, Evidence for kinetic effects on shock wave metamorphism: Laboratory experiments compared with inferences from studies of natural impact craters, *Lunar Planet. Sci.*, *XXXII*, 1822, 2001.
Dence, M. R., R. A. F. Grieve, and P. B. Robertson, Terrestrial impact structures: Principal characteristics and energy considerations, in *Impact and Explosion Cratering*, edited by D. J. Roddy, R. O. Pepin, and R. B. Merrill, pp. 247–275, Pergamon, New York, 1977.
Dundon, R. W., and S. S. Hafner, Cation disorder in shocked orthopyroxene, *Science*, *174*, 581–583, 1971.
Duvall, G. E., Concepts of shock wave propagation, *Bull. Seismol. Soc. Am.*, *4*, 869–893, 1962.
Estep, P. A., J. J Kovach, P. Waldstein, and C. Karr Jr., Infrared and Raman spectroscopic studies of structural variations in minerals from Apollo 11, 12, 14, and 15 samples, *Proc. Lunar Planet. Sci. Conf. 3rd* (Suppl. 3, *Geochim. Cosmochim. Acta*), 3047–3067, 1972.
Feldman, V., S. Kotelnickov, L. Sazonova, and E. Guseva, Diaplectic transformation in clinopyroxene (Puchezh-Katunky astrobleme, Russia), *Lunar Planet. Sci.*, *XXV*, 369–370, 1994.
Friedman, R. C., G. J. Taylor, and A. Treiman, Processes in thick lava flows: Nakhlites (Mars) and Theo's Flow (Ontario, Earth), *Lunar Planet. Sci.*, *XXVI*, 429–430, 1995.
Garvin, J. B., C. C. Schnetzler, and R. A. F. Grieve, Characteristics of large terrestrial impact structures as revealed by remote sensing studies, *Tectonophysics*, *216*, 45–62, 1992.
Gibbons, R. V., R. V. Morris, F. Hörz, and T. D. Thompson, Petrographic and ferromagnetic resonance studies of experimentally shocked regolith analogs, *Proc. Lunar Sci. Conf. 6th*, 3143–3171, 1975.
Grieve, R. A. F., F. Langenhorst, and D. Stöffler, Shock metamorphism of quartz in nature and experiment, II, Significance in geoscience, *Meteorol. Planet. Sci.*, *31*, 6–35, 1996.
Hamilton, V. E., Thermal infrared emission spectroscopy of the pyroxene mineral series, *J. Geophys. Res.*, *105*, 9701–9716, 2000.
Hamilton, V. E., and P. R. Christensen, Determining the model mineralogy of mafic and ultramafic igneous rocks using thermal emission spectroscopy, *J. Geophys. Res.*, *105*, 9717–9734, 2000.
Hamilton, V. E., P. R. Christensen, and H. Y. McSween Jr., Determination of Martian meteorite lithologies and mineralogies using vibrational spectroscopy, *J. Geophys. Res.*, *102*, 25,593–25,603, 1997.
Hamilton, V. E., M. B. Wyatt, H. Y. McSween Jr., and P. R. Christensen, Analysis of terrestrial and Martian volcanic compositions using thermal emission spectroscopy, 2, Application to Martian surface spectra from the Mars Global Surveyor Thermal Emission Spectrometer, *J. Geophys. Res.*, *106*, 14,733–14,746, 2001.
Hanss, R. E., B. R. Montague, M. K. Davis, C. Galindo, and F. Hörz, X-ray diffractometer studies of shocked minerals, *Proc. Lunar Planet. Sci. Conf. 9th*, 2773–2787, 1978.
Hartmann, W. K., M. Malin, A. McEwen, M. Carr, L. Soderblom, P. Thomas, E. Danielson, P. James, and J. Veverka, Evidence for recent volcanism on Mars from crater counts, *Nature*, *397*, 586–589, 1999.
Haskin, L. A., and P. A. Salpas, Genesis of compositional characteristics of Stillwater AN-I and AN-II thick anorthositic units, *Geochim. Cosmochim. Acta*, *56*, 1187–1212, 1992.
Henderson, B. G., and B. M. Jakosky, Near-surface thermal gradients and their effects on mid-infrared emission spectra of planetary surfaces, *J. Geophys. Res.*, *99*, 19,063–19,073, 1994.
Hess, H. H., Stillwater igneous complex, Montana: A quantitative mineralogical study, *Mem. Geol. Soc. Am.*, *80*, 230 pp., 1960.
Heymann, D., and F. Hörz, Raman-spectroscopy and X-ray diffractometer studies of experimentally produced diaplectic feldspar glass, *Phys. Chem. Miner.*, *17*, 38–44, 1990.
Hoefen, T. M., and R. N. Clark, Compositional variability of Martian olivines using Mars Global Surveyor thermal emission spectra, *Lunar Plan. Sci.*, *XXXII*, abstract 2049, 2001.
Hofmeister, A. M., Infrared reflectance spectra of fayalite, and absorption data from assorted olivines, including pressure and isotope effects, *Phys. Chem. Miner.*, *24*, 535–546, 1997.
Hofmeister, A. M., J. Xu, H.-K. Mao, P. M. Bell, and T. C. Hoering, Thermodynamics of Fe-Mg olivines at mantle pressures: Mid- and far-infrared spectroscopy at high pressure, *Am. Mineral.*, *74*, 281–306, 1989.
Horton, K. H., S. K. Sharma, N. Domergue-Schmidt, and P. G. Lucey, Performance of a CW-laser remote raman system, *Lunar Planet. Sci.*, *XXXII*, abstract 1462, 2001.
Hörz, F., Statistical measurements of deformation structures and refractive indices in experimentally shock loaded quartz, in *Shock Metamorphism of Natural Materials: Proceedings*, pp. 243–253, Mono Book, Baltimore, Md., 1968.
Hörz, F., and M. Cintala, Impact experiments related to the evolution of planetary regoliths, *Meteorol. Planet. Sci.*, *32*, 179–209, 1997.
Hörz, F., and W. L. Quaide, Debye-Scherrer investigations of experimentally shocked silicates, *Moon*, *6*, 45–82, 1973.
Hörz, F., D. W. Mittlefehldt, T. H. See, and C. Galindo, Petrographic studies of the impact melts from Meteor Crater, AZ, *Meteorit. Planet. Sci.*, *37*, 501–531, 2002.
Iiishi, K., T. Tomisaka, T. Kato, and Y. Umegaki, Isomorphous substitution and infrared and far infrared spectra of the feldspar group, *Neues Jahrb. Mineral. Abh.*, *115*, 98–119, 1971.
Jackson, E. D., Primary textures and mineral associations in the ultramafic zone of the Stillwater Complex Montana, *U.S. Geol. Surv. Prof. Pap.*, *348*, 1961.
Johnson, J. R., P. G. Lucey, K. A. Horton, and E. M. Winter, Infrared measurements of pristine and disturbed soils, 1, Spectral contrast differences between field and laboratory data, *Remote Sens. Environ.*, *64*, 34–46, 1998.
Johnson, J. R., M. I. Staid, and T. N. Titus, Shocked plagioclase signatures in Thermal Emission Spectrometer data of Mars, *Lunar Planet Sci.*, *XXXIII*, abstract 1345, 2002.
Jones, A. H., W. M. Isbell, and J. C. Maiden, Measurements of the very-high-pressure properties of materials using a light-gas gun, *J. Appl. Phys.*, *37*, 3493–3499, 1966.
King, T. V. V., Contributions toward a quantitative understanding of reflectance spectroscopy: Phyllosilicates, olivine and shocked materials, Ph.D. dissertation, 230 pp., Univ. of Hawaii, Honolulu, 1986.
Kotelnikov, S., and V. I. Feldman, Experimental study of shock metamorphism in clinopyroxene, *Geol. Bull. Moscow Univ.*, *53*, 37–41, 1998.
Lambert, P., Reflectivity applied to peak pressure estimates in silicates of shocked rocks, *J. Geophys. Res.*, *86*, 6187–6204, 1981.
Lambert, P., Shock experiments in pyroxenes, and some of their alteration products, *Meteoritics*, *1*, 241, 1982.
Langenhorst, F., Experimentally shocked plagioclase: Changes of refractive indices and optic axial angle in the 10–30 GPa range, *Meteoritics*, *24*, 291, 1989.
Leroux, H., J. C. Doukhan, and F. Langenhorst, Microstructural defects in experimentally shocked diopside: A TEM characterization, *Phys. Chem Miner.*, *20*, 521–530, 1994.
Lucey, P. G., Radiative transfer model constraints on the shock state of remotely sensed lunar anorthosites, *Geophys. Res. Lett.*, 1486, doi:10.1029/2001GL014655, 2002.
Lyon, R. J. P., Evaluation of infrared spectrophotometry for compositional analysis of lunar and planetary soils, *NASA Tech. Note D-1871*, 1963.
Marsh, S. P., *LASL Shock Hugoniot Data*, 658 pp., Univ. of Calif. Press, Berkeley, 1980.
McSween, H. Y., What we have learned about Mars from SNC meteorites, *Meteoritics*, *29*, 757–779, 1994.
Mikouchi, T., Shocked plagioclase in the lunar meteorites Yamato-793169 and Asuka-881757: Implications for their shock and thermal histories, *Antarct. Meteorite Res.*, *12*, 151–167, 1999.
Morris, P. W., A. M. Heras, B. Vandenbussche, and R. Dijkstra, Asteroid 4 Vesta as seen with the infrared space observatory short wavelength spectrometer, *LPI Contrib. 969*, pp. 19–20, Lunar and Planet. Inst., Houston, Tex., 1999.
Mustard, J. F., and J. E. Hays, Effects of hyperfine-particles on reflectance spectra from 0.3 to 25 μm, *Icarus*, *125*, 145–163, 1997.
Nash, D. B., and J. W. Salisbury, Infrared reflectance spectra (2.2–15 μm) of plagioclase feldspars, *Geophys. Res. Lett.*, *18*, 1151–1154, 1991.
Nash, D. B., J. W. Salisbury, J. E. Conel, P. G. Lucey, and P. R. Christensen, Evaluation of infrared emission spectroscopy for mapping the Moon's surface composition from lunar orbit, *J. Geophys. Res.*, *98*, 23,535–23,552, 1993.

Nyquist, L. E., D. D. Bogard, C.-Y. Shih, A. Greshake, D. Stöffler, and O. Eugster, Ages and geologic histories of Martian meteorites, in *Chronology and Evolution of Mars*, *Space Sci. Rev.*, *96*, 105–164, 2001.

Ostertag, R., Shock experiments on feldspar crystals, *Proc. Lunar Planet. Sci. Conf. 14th*, Part 1 *J. Geophys. Res.*, *88*, suppl., B364–B376, 1983.

Page, N. J., Stillwater complex, Montana: Rock succession, metamorphism and structure of the complex and adjacent rocks, *U.S. Geol. Surv. Prof. Pap.*, *999*, 79 pp., 1977.

Papike, J. J., M. N. Spilde, G. W. Fowler, and I. S. McCallum, SIMS studies of planetary cumulates: Orthopyroxene from the Stillwater Complex, Montana, *Am. Mineral.*, *80*, 1208–1221, 1995.

Pollack, S. S., and P. S. DeCarli, Enstatite: Disorder produced by a megabar shock event, *Science*, *165*, 591–592, 1969.

Raedeke, L. D., and I. S. McCallum, Investigations in the Stillwater Complex: part II, Petrology and petrogenesis of the ultramafic series, *J. Petrol.*, *25*, 395–420, 1984.

Ramsey, M. S., and P. R. Christensen, Ejecta patterns of Meteor Crater, Arizona, derived from the linear un-mixing of TIMS data and laboratory thermal emission spectra, in *Summary of the Third Annual Airborne Geoscience Workshop*, vol. 2, *TIMS Workshop*, edited E. A. Abbott, *JPL Publ. 92-14*, pp. 34–36, Jet Propul. Lab., Pasadena, Calif., 1992.

Ramsey, M. S., and P. R. Christensen, Mineral abundance determination: Quantitative deconvolution of thermal emission spectra, *J. Geophys. Res.*, *103*, 577–596, 1998.

Reynard, B., M. Okuno, Y. Shimada, Y. Syono, and C. Willaime, A Raman spectroscopic study of shock-wave densification of anorthite ($CaAl_2Si_2O_8$) glass, *Phys. Chem. Miner.*, *26*, 432–436, 1999.

Ruff, S. W., and P. R. Christensen, Bright and dark regions on Mars: Particle size and mineralogical characteristics based on Thermal Emission Spectrometer data, *J. Geophys. Res.*, *107*, XXXX, doi:10.1029/2001JE001580, in press, 2002.

Ruff, S. W., P. R. Christensen, P. W. Barbera, and D. L. Anderson, Quantitative thermal emission spectroscopy of minerals: A technique for measurement and collection, *J. Geophys. Res.*, *102*, 14,899–14,913, 1997.

Salisbury, J. W., Mid-infrared spectroscopy: Laboratory data, in *Remote Geochemical Analysis*, edited by C. Pieters and P. Englert, chap. 4, pp. 79–98, Cambridge Univ. Press, New York, 1993.

Salisbury, J. W., and A. Wald, The role of volume scattering in reducing spectral contrast of reststrahlen bands in spectra of powdered minerals, *Icarus*, *96*, 121–128, 1992.

Salisbury, J. W., and L. S. Walter, Thermal infrared (2.5–13.5 μm) spectroscopic remote sensing of igneous rock types on particulate planetary surfaces, *J. Geophys. Res.*, *94*, 9192–9202, 1989.

Salisbury, J. W., D. M. D'Aria, and E. Jarosewich, Midinfrared (2.5–13.5 μm) reflectance spectra of powdered stony meteorites, *Icarus*, *92*, 280–297, 1991a.

Salisbury, J. W., L. S. Walter, N. Vergo, and D. M. D'Aria, *Infrared (2.1–25 μm) Spectra of Minerals*, 267 pp., Johns Hopkins Univ. Press, Baltimore, Md., 1991b.

Salisbury, J. W., A. Wald, and D. M. D'Aria, Thermal-infrared remote sensing and Kirchhoff's law, 1, Laboratory measurements, *J. Geophys. Res.*, *99*, 11,897–11,911, 1994.

Salisbury, J. W., D. G. Murcray, W. J. Williams, and R. D. Blatherwick, Thermal infrared spectra of the Moon, *Icarus*, *115*, 181–190, 1995.

Salisbury, J. W., A. Basu, and E. M. Fischer, Thermal infrared spectra of lunar soils, *Icarus*, *130*, 125–139, 1997.

Sazonova, L., E. Kozlov, and Y. Zhugin, Transformations of quartz-plagioclase-garnet-clinopyroxene rock in spherical stress waves, *Lunar Planet. Sci.*, *XXVII*, 1135–1136, 1996.

Schmitt, R. T., and A. Deutsch, X-ray investigation of olivine and orthopyroxene in experimentally shocked samples of the H6-chondrite Kernouvé, *Lunar Planet. Sci.*, *XXI*, 1243–1244, 1995.

Schneider, H., Infrared spectroscopic studies of experimentally shock-loaded quartz, *Meteoritics*, *13*, 227–234, 1978.

Schneider, H., and U. Hornemann, Preliminary data on the shock-induced high-pressure transformation of olivine, *Earth Planet. Sci. Lett.*, *36*, 322–324, 1977.

Schultz, P. H., and J. M. Mustard, Martian impact glass: generation and evidence, *Lunar Plan. Sci.*, *XXIX*, abstract 1847, 1998.

Short, N. M., Progressive shock metamorphism of quartzite ejecta from the Sedan nuclear explosion crater, *J. Geol.*, *78*, 705–732, 1970.

Squyres, S. W., et al., The Athena Mars rover science payload, *Lunar Planet. Sci.*, *XXIX*, abstract 1101, 1998.

Sprague, A. L., F. C. Witteborn, R. W. H. Kozlowski, D. P. Cruikshank, M. J. Bartholomew, and A. L. Graps, The Moon: Mid-infrared (7.5-to 11.4-μm) spectroscopy of selected regions, *Icarus*, *100*, 73–84, 1992.

Sprague, A. L., R. W. H. Kozlowski, F. C. Witteborn, D. P. Cruikshank, and D. H. Wooden, Mercury: Evidence for anorthosite and basalt from mid-infrared (7.3–13.5 μm) spectroscopy, *Icarus*, *109*, 156–167, 1994.

Stöffler, D., Deformation and transformation of rock-forming mineral by natural and experimental shock processes, I, Behavior of minerals under shock compression, *Forschr. Miner.*, *49*, 50–113, 1972.

Stöffler, D., Deformation and transformation of rock-forming minerals by natural and experimental shock processes, II, Physical properties of shocked minerals, *Forschr. Miner.*, *51*, 256–289, 1974.

Stöffler, D., Maskelynite confirmed as diaplectic glass: Indication for peak shock pressures below 45 GPa in all Martian meteorites, *Lunar Planet. Sci.*, *XXXII*, abstract 1170, 2001.

Stöffler, D., and U. Hornemann, Quartz and feldspar glasses produced by natural and experimental shock, *Meteoritics*, *7*, 371–394, 1972.

Stöffler, D., and F. Langenhorst, Shock metamorphism of quartz in nature and experiment, I, Basic observation and theory, *Meteoritics*, *29*, 155–181, 1994.

Stöffler, D., K. Keil, and E. Scott, Shock metamorphism of ordinary chondrites, *Geochim. Cosmochim. Acta*, *55*, 3845–3867, 1991.

Strom, R. G., S. K. Croft, and N. G. Barlow, The Martian impact cratering record, in *Mars*, chap. 12, pp. 383–423, Univ. of Ariz. Press, Tucson, 1992.

Thomson, J., and J. Salisbury, The mid-infrared reflectance of mineral mixtures (7–14μm), *Remote Sens. Environ.*, *45*, 1–13, 1993.

Treiman, A. H., M. Norman, D. Mittlefehldt, and J. Crisp, "Nakhlites" on Earth: Chemistry of clinopyroxenites from Theo's Flow,Ontario, Canada, *Lunar Planet. Sci.*, *XXVII*, 1341–1342, 1996.

Velde, B., and H. Boyer, Raman microprobe spectra of naturally shocked microcline feldspars, *J. Geophys. Res.*, *90*, 3675–3682, 1985.

Velde, B., Y. Syono, R. Couty, and M. Kikuchi, High pressure infrared spectra of diaplectic anorthite glass, *Phys. Chem. Miner.*, *14*, 345–349, 1987.

Velde, B., Y. Syono, M. Kikuchi, and H. Boyer, Raman microprobe study of synthetic diaplectic plagioclase feldspars, *Phys. Chem. Miner.*, *16*, 436–441, 1989.

Wang, A., B. L. Jolliff, and L. A. Haskin, Raman spectroscopic characterization of a highly weathered basalt; igneous mineralogy, alteration products, and a microorganism, *J. Geophys. Res.*, *104*, 27,067–27,077, 1999.

Wang, S. Y., S. K. Sharma, and T. F. Cooney, Micro-Raman and infrared spectral study of forsterite under high pressure, *Am. Mineral.*, *78*, 469–476, 1993.

Williams, Q., High-pressure infrared spectra of feldspars: Constraints on compressional behavior, amorphization, and diaplectic glass formation, in *Properties of Earth and Planetary Material at High Pressure and Temperature, Geophys. Monogr. Ser.*, vol. 101, edited by M. H. Manghnani and T. Yagi, pp. 531–543, AGU, Washington, D.C., 1998.

Williams, Q., and R. Jeanloz, Spectroscopic evidence for pressure-induced coordination changes in silicate glasses and melts, *Science*, *239*, 902–905, 1988.

Williams, Q., and R. Jeanloz, Static amorphization of anorthite at 300K and comparison with diaplectic glass, *Nature*, *338*, 413–415, 1989.

Wyatt, M. B., V. E. Hamilton, H. Y. McSween Jr., P. R. Christensen, and L. A. Taylor, Analysis of terrestrial and Martian volcanic compositions using thermal emission spectroscopy, I, Determination of mineralogy, chemistry, and classification strategies, *J. Geophys. Res.*, *106*, 14,711–14,732, 2001.

Xie, X., M. Chen, C. Dai, A. El Goresy, and P. Gillet, A comparative study of naturally and experimentally shocked chondrites, *Earth Planet. Sci. Lett.*, *187*, 345–356, 2001.

Yamaguchi, A., and T. Sekine, Monominerallic mobilization of plagioclase by shock: An experimental study, *Earth. Planet. Sci. Lett.*, *175*, 289–296, 2000.

P. R. Christensen, Department of Geology, Arizona State University, Tempe, AZ 85287-1404, USA.

F. Hörz, Johnson Space Center, Houston, TX, USA.

J. R. Johnson, U.S. Geological Survey, 2255 North Gemini Drive, Flagstaff, AZ 86001, USA. (jrjohnson@usgs.gov)

P. G. Lucey, Hawaii Institute of Geophysics and Planetology, University of Hawaii, 2525 Correa Road, Honolulu, HI 96822, USA.